

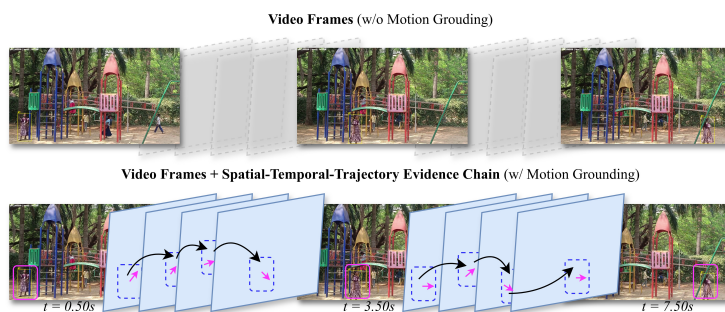
Motion-o: Trajectory-Grounded Video Reasoning

Bishoy Galoaa*, Shayda Moezzi*, Xiangyu Bai, and Sarah Ostadabbas

Northeastern University, Boston, MA, USA

{galoaa.b, moezzi.s, bai.xiang, s.ostadabbas}@northeastern.edu

*These authors contributed equally to this work.



❓ What is the girl's trajectory across the playground?

Ground Truth Answer: The girl walks from the left side of the frame, passes in front of the jungle gym, and exits on the right side of the frame.

Motion-o

```
<think>The video begins with the <obj>girl</obj><box>[0.05, 0.68, 0.13, 0.97]</box>at<t>0.5</t> appearing on the left side of the frame, wearing a purple and white patterned dress. She then walks from left to right, and by the midpoint of her journey, the <obj>girl</obj><box>[0.0469, 0.6935, 0.1214, 0.9991]</box>at<t>1.5</t> <obj>girl</obj><box>[0.1354, 0.6954, 0.2266, 0.9991]</box>at<t>2.5</t><obj>girl</obj><box>[0.3, 0.69, 0.38, 1.0]</box>at<t>3.5</t> is seen in the center of the frame, passing in front of the jungle gym. Continuing her path, the <obj>girl</obj><box>[0.4411, 0.6843, 0.5234, 0.9991]</box>at<t>4.5</t> <obj>girl</obj><box>[0.5771, 0.6991, 0.6771, 0.9991]</box>at<t>5.5</t> <obj>girl</obj><box>[0.6964, 0.7222, 0.7849, 0.9991]</box>at<t>6.5</t><obj>girl</obj><box>[0.82, 0.72, 0.9, 1.0]</box>at<t>7.5</t><motion obj="girl" dir="E" speed="fast" scale="stable"/> reaches the right side of the frame and proceeds to walk out of view, completing her traversal of the scene.</think>
```

Motion Chain of Thought (MCoT)

Qwen2.5-VL-7B

```
<think>The girl starts by walking towards the playground structure on the left side of the frame. She then moves across the playground, passing through the middle area before heading towards the right side of the frame. Her movement appears to be continuous and directed, indicating she is exploring the playground. The girl's trajectory can be described as follows: - Initially, she walks towards the left side of the playground. - She then crosses the middle area of the playground. - Finally, she heads towards the right side of the frame.</think>
```

Baseline Chain of Thought

Fig. 1: Motion-o: trajectory-grounded video reasoning. Although recent video models can produce fluent `<think>` traces, their reasoning is typically ungrounded, it does not explicitly tie claims back to where/when evidence occurs in the video, nor does it encode the motion that connects observations. Motion-o introduces a **Spatial-Temporal-Trajectory (STT) evidence chain**: timestamped `<obj, box, t>` observations paired with a structured `<motion/>` tag that explicitly links snapshots into a trajectory-faithful trace.

Abstract. Recent research has made substantial progress on video reasoning, with many models leveraging spatio-temporal evidence chains to strengthen their inference capabilities. At the same time, a growing set of datasets and benchmarks now provides structured annotations designed to support and evaluate such reasoning. However, little attention has been paid to reasoning about *how* objects move between observations:

no prior work has articulated the motion patterns by connecting successive observations, leaving trajectory understanding implicit and difficult to verify. We formalize this missing capability as Spatial-Temporal-Trajectory (STT) reasoning and introduce **Motion-o**, a motion-centric video understanding extension to visual language models that makes trajectories explicit and verifiable. To enable motion reasoning, we also introduce a trajectory-grounding dataset artifact that expands sparse keyframe supervision via augmentation to yield denser bounding box tracks and a stronger trajectory-level training signal. Finally, we introduce Motion Chain of Thought (MCoT), a structured reasoning pathway that makes object trajectories through discrete `<motion/>` tag summarizing per-object direction, speed, and scale (of velocity) change to explicitly connect grounded observations into trajectories. To train Motion-o, we design a reward function that compels the model to reason directly over visual evidence, all while requiring no architectural modifications. Empirical results demonstrate that Motion-o improves spatial-temporal grounding and trajectory prediction while remaining fully compatible with existing frameworks, establishing motion reasoning as a critical extension for evidence-based video understanding. Code is available at <https://github.com/ostadabbas/Motion-o>.

Keywords: Video Understanding · Motion Reasoning · Reinforcement Learning · Chain-of-Thought

1 Introduction

Humans effortlessly perceive motion; we recognize when a person walks leftward, when a ball accelerates, or when a vehicle follows a smooth arc. This capacity for motion understanding is so fundamental that it often goes unnoticed, yet it underpins our ability to predict, explain, and reason about the dynamic visual world. By contrast, today’s vision-language models (VLMs) still lack an explicit mechanism to reason about how objects move between observations. As a result, models frequently rely on static priors or textual interpolation to “fill in” dynamics, producing motion statements that are plausible but ungrounded and difficult to verify.

As illustrated in the bottom example of Figure 1, many video reasoning models produce free-form rationales that are not required to cite explicit spatial or temporal evidence (e.g., where an object is, and when). This makes the reasoning trace weakly grounded: correct answers may rely on static priors rather than verifiable observations. Recent advances in video understanding [5, 13, 20] has substantially improved **when** and **where** models can ground evidence in video. A growing line of work trains models to emit structured evidence chains: sequences of timestamped bounding boxes that localize objects across frames. As illustrated in the top example in Figure 2, spatio-temporal evidence chains provide grounded *snapshots*—i.e., an `<obj>` with `<box>` coordinates at timestamps [13]—but they leave the inter-frame dynamics implicit. In other words, they specify *where* an entity is at a few moments, while the model must implic-

itly interpolate *how* it moved between observations. The missing link is motion: a structured relation across time involving direction, velocity, and scale change. Without an explicit motion representation, models must infer trajectories implicitly, which makes trajectory understanding hard to interpret, easy to shortcut with priors, and difficult to evaluate directly [12, 17, 24].

This gap matters more than it might appear. Full video comprehension requires what we term Spatial-Temporal-Trajectory (STT) Reasoning: the joint capacity to reason about *where* objects are (spatial), *when* they appear (temporal), and *how* they move between observations (trajectory). Existing evidence-based frameworks largely address the first two dimensions but leave the third entirely implicit. Yet trajectory reasoning is not merely interpolation between boxes; it requires reasoning about direction, velocity, and acceleration. Knowing that a person appeared at position A at time t_1 and position B at time t_2 is necessary but insufficient. What is often needed is an explicit articulation such as: moved leftward at moderate speed while approaching the camera, or remained stationary, or followed a smooth arc. These descriptors provide the semantic glue that connects observations into a coherent trajectory and enables downstream capabilities such as trajectory prediction, anomaly detection, and motion-sensitive question answering (e.g., “Which direction did the person walk?”).

We introduce **Motion-o**, a motion-centric extension to grounded video reasoning that makes trajectory understanding explicit and rewardable, without requiring architectural changes. Motion-o builds on spatio-temporal evidence chains and adds a lightweight but crucial operator: a structured Motion Chain of Thought (MCoT) step that forces the model to summarize motion between grounded observations. Concretely, after the model grounds an object at multiple timestamps it must emit a self-closing `<motion/>` tag that describes the trajectory connecting those observations. Each motion tag contains discrete, interpretable attributes including direction, speed, and scale change. For example, “`<motion obj="person" dir="W" speed="slow" scale="stable"/>`.” This creates an explicit intermediate step that bridges spatial snapshots to continuous dynamics, turning implicit motion into a structured statement. Figure 1 provides an overview how we inject motion as an explicit, ver-

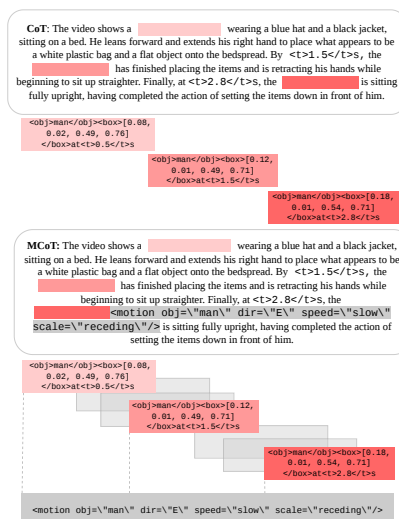


Fig. 2: CoT vs. Motion Chain-of-Thought (MCoT). CoT in [13] yields sparse temporal bounding boxes, forcing implicit inter-frame interpolation. MCoT adds an object-conditioned `<motion/>` tag that explicitly parameterizes the dynamics between observations, making the evidence chain trajectory-consistent and reducing prior-driven extrapolation.

ifiable intermediate into grounded video reasoning, while Figure 2 isolates the key mechanism: the `<motion/>` tag that bridges successive spatio-temporal observations, converting a snapshot-based evidence chain into a spatial-temporal-trajectory reasoning trace.

A key challenge is supervision; existing grounding datasets provide sparse key-frames, while motion is inherently defined over continuous time [11,13,21]. To address this, we introduce a trajectory-grounding dataset artifact that expands sparse keyframe supervision with denser bounding box tracks suitable for motion supervision. From these tracks, we compute discrete motion primitives (direction, speed, and scale-change) automatically and inject them into reasoning traces during supervised fine-tuning, teaching the model the MCoT schema. We then reinforce motion reasoning with trajectory-grounded rewards during reinforcement learning. Motion-o uses two complementary signals: (i) a trajectory reward that measures agreement between predicted motion tags and ground-truth motion derived from tracks, and (ii) a visual grounding reward based on dual-chain verification that penalizes motion descriptions that remain unchanged when temporal motion cues are removed (e.g., by freezing frames). Together, these rewards suppress two common failure modes in video understanding: producing motion narratives that do not align with the visual trajectory, and defaulting to motion claims that remain unchanged when temporal evidence is removed.

Our contributions are as follows: (1) **Motion-o**, a motion-centric extension for grounded video reasoning that makes object trajectories explicit and verifiable by augmenting evidence chains with structured motion descriptors. (2) We formalize **Spatial-Temporal-Trajectory (STT) reasoning**, identifying trajectory understanding—how objects move between observations—as a missing capability in current video reasoning frameworks. (3) We introduce **Motion Chain of Thought (MCoT)**, a structured reasoning step that summarizes direction, speed, and scale change through discrete `<motion/>` tags, enabling interpretable trajectory reasoning without modifying model architectures. (4) We develop a trajectory-grounded training framework that expands sparse keyframe supervision with dense bounding box tracks and trains motion reasoning using trajectory-aware rewards, improving spatial-temporal grounding and trajectory prediction while remaining fully compatible with existing VLM pipelines.

2 Related Work

Spatial and Temporal Video Reasoning. Recent advances in LLMs and VLMs equip them with mechanisms to build and manipulate structured intermediate representations, allowing them to reason through multi-step transformations rather than relying solely on pattern matching or next-token prediction. A growing body of work seeks to extend visual reasoning into video understanding, with particular focus on identifying *when* and *where* relevant evidence appears within a sequence. These efforts approach the problem from complementary

angles, reflecting the central role of temporal and spatial localization in video reasoning. On the temporal side, Time-R1 [21] introduces verifiable rewards for temporal grounding with strong generalization, and TVG-R1 [2] improves robustness through curated datasets. On the spatial side, SpaceR [15] leverages RL for object-centric grounding and geometric reasoning. Open-o3 Video [13] unifies both dimensions, generating timestamped frames with localized bounding boxes as structured evidence. However, all of these methods focus on *where objects are located* rather than *how they move*. While motion metrics appear as rewards in some systems [13], the models themselves never articulate motion patterns in their reasoning. Our work addresses precisely this gap, making trajectory reasoning an explicit part of the model’s output.

Evidence-based Video Reasoning. Rather than directly reason over high-dimension visual patches, a parallel body of work [4, 7, 19, 26] investigates how to utilize explicit visual operations such as detection, segmentation and tracking. DeepEyes [26] shows that end-to-end RL can incentivize image-tool reasoning, and TreeBench [18] provides methodology for traceable, box-level evidence in images. In the video domain, OpenAI-o3 [14] formalizes the notion of “thinking with images,” and Open-o3 Video [13] extends this idea to “thinking with frames,” emitting timestamped crops and bounding boxes, while STVG-o1 [7] introduces a bounding box chain-of-thought for spatio-temporal grounding. These approaches compellingly demonstrate the value of explicit evidence, yet they focus almost exclusively on spatial localization. *Motion*—the temporal evolution of spatial positions—remains implicit throughout. Our Motion Chain of Thought explicitly bridges successive temporal observations with trajectory reasoning, adding the missing dynamic dimension to evidence-based video understanding.

The Motion Reasoning Gap. Despite parallel advances in temporal grounding (when), spatial grounding (where), and evidence-based reasoning (what), no existing method achieves full Spatial-Temporal-Trajectory Reasoning—explicitly reasoning about *how* objects move. Some works [13, 15] incorporate motion metrics as implicit training signals, but the models never learn to *articulate* the motion patterns they rely on. This makes trajectory reasoning opaque—both to users seeking explanations and to the models themselves during inference.

Reinforcement Learning-based training. Existing works leverage RL to push video understanding beyond direct reasoning to spatio-temporal evidence reasoning. Video-R1 [5] demonstrates that temporal-aware GRPO with curated reasoning data substantially improves video understanding, while VideoChat-R1 [11] extends this to spatio-temporal perception without degrading QA performance. More recently, Video-RTS [23] combines RL with test-time scaling, and DeepVideo-R1 [16] introduces difficulty-aware regularization to better exploit temporal structure. These works establish RL as a powerful paradigm for video reasoning but operate primarily over textual outputs.

With RL, Motion-o reshapes video reasoning by making motion an explicit and structured element of the inference process, effectively closing the gap left by models that treat motion only as an implicit or secondary cue. We introducing Motion Chain of Thought, which elevates trajectory reasoning from an implicit

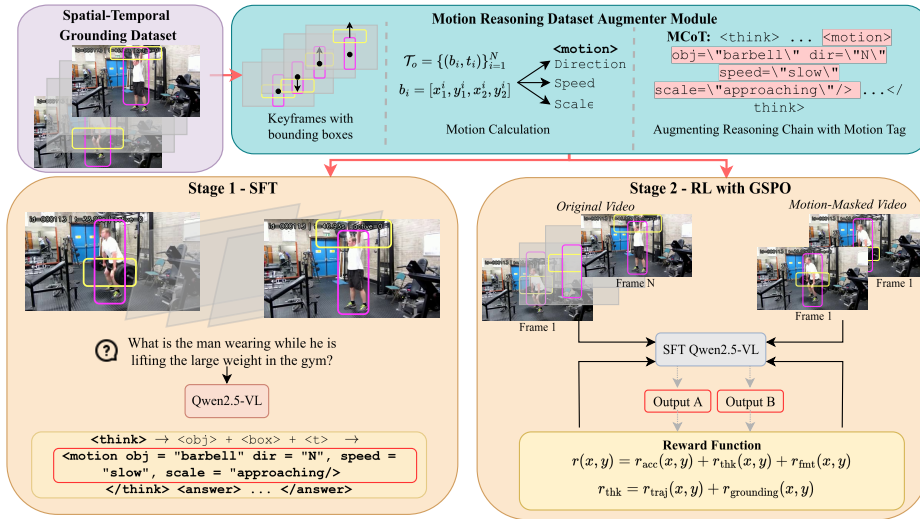


Fig. 3: Motion-o end-to-end pipeline. Starting from the spatio-temporal grounding dataset from [13] with keyframe boxes plus the addition of our dense interpolated bounding boxes (purple box), we (i) compute track-derived motion primitives (direction/speed/scale) and inject them into the reasoning trace as an MCoT `<motion/>` tag (blue box), (ii) perform supervised fine-tuning (Stage 1) to teach the model the structured STT/MCoT format, and (iii) perform RL (GSPO) (Stage 2) with original vs. motion-masked videos to reward motion tags that align with trajectories and change when temporal evidence is removed.

training signal to an explicit, verifiable component of the model’s output, completing the spatial-temporal-trajectory triad and pushing video understanding toward more structured, interpretable reasoning.

3 Introducing Motion-o

We present Motion-o, a framework that extends grounded video reasoning with an explicit trajectory reasoning step (Figure 3). Existing evidence-based video reasoning methods [7, 13] generate verifiable spatio-temporal observations (objects, boxes, timestamps), but typically leave the motion that connects the observations implicit. Motion-o closes this gap by augmenting spatio-temporal evidence chains with a discrete `<motion/>` descriptor that summarizes how an object moves between grounded observations.

Given a video-question pair (\mathcal{V}, q) , the model outputs

$$y = \langle \text{think} \rangle R \langle / \text{think} \rangle \langle \text{answer} \rangle A \langle / \text{answer} \rangle,$$

where R contains (i) grounded spatio-temporal evidence and (ii) explicit motion descriptors. Motion-o is trained in two stages: (i) supervised fine-tuning (SFT) on motion-augmented reasoning traces that teach the model the structured format

and syntax, and (ii) reinforcement learning that directly optimizes motion-centric rewards to encourage accurate and visually grounded motion descriptions.

Corresponding with Figure 3, we first summarize the spatio-temporal evidence format that we extend to Spatial-Temporal-Trajectory evidence (Sec. 3.1), then introduce MCoT and how we obtain supervision for motion tags (Sec. 3.2), and finally describe the training pipeline and trajectory-grounded rewards (Sec. 3.3).

3.1 Spatial-Temporal-Trajectory (STT) Evidence Chains

Following Open-o3 Video [13], we adopt a structured format for grounding reasoning in visual evidence. Given a video \mathcal{V} and question q , the model produces a response organized as $\langle \text{think} \rangle R \langle / \text{think} \rangle \langle \text{answer} \rangle A \langle / \text{answer} \rangle$, where R contains the reasoning trace and A the final answer. Within R , each grounded claim is written as:

$$\langle \text{obj} \rangle o \langle / \text{obj} \rangle \langle \text{box} \rangle b \langle / \text{box} \rangle \text{ at } \langle \text{t} \rangle t \langle / \text{t} \rangle \text{s}, \quad (1)$$

where o is the object name, $b = [x_1, y_1, x_2, y_2]$ is a normalized bounding box, and t is the timestamp in seconds. This representation creates an evidence chain that anchors language to concrete observations across time. For example, a model might write: “The man is visible holding a glass at 47.5s, and later at 54.2s is smiling,” each claim anchored by a precise spatial location and timestamp. However, even when the same object is referenced at multiple timestamps, the evidence chain remains a set of discrete snapshots: it specifies where the object was at t_1 and t_2 , but leaves the trajectory dynamics between t_1 and t_2 implicit. Motion-o targets precisely this missing link.

3.2 Motion Chain of Thought (MCoT)

We extend spatio-temporal evidence chains with explicit motion reasoning via a self-closing `<motion/>` tag to create spatial-temporal-trajectory evidence chains. The core idea is: after the model generates multiple temporal observations of the same object, it must summarize the motion that connects them. This converts a sequence of grounded boxes into a minimal, structured trajectory descriptor that is both interpretable and rewardable. so for

Motion Tag Format Each `<motion/>` tag carries discrete attributes: *obj* (object name), *dir* (direction: N, NE, E, SE, S, SW, W, NW, or STAT for stationary), *speed* (stationary, slow, moderate, fast), and *scale* (approaching, stable, receding). The format is:

$$\langle \text{motion } \text{obj} = \textit{name} \text{ dir} = \textit{D} \text{ speed} = \textit{S} \text{ scale} = \textit{C} \text{ /} \rangle. \quad (2)$$

Unified Reasoning Flow. The complete reasoning chain then integrates temporal observations, spatial grounding, and motion reasoning into a single sequence. This enforces an explicit pathway: observe the object at multiple timestamps, ground each observation in a bounding box, emit a structured motion

summary that links observations into a trajectory, and use that trajectory information to support the final answer. Importantly, the `<motion/>` is not an extra token, it is an intermediate reasoning operator that makes trajectory understanding explicit and verifiable.

Automatic Motion Computation. To teach MCoT without additional human annotation, we generate discrete motion primitives directly from the bounding boxes provided in each sample in the STGR dataset [13]. Using the provided keyframe timestamps and object bounding boxes, we group bounding boxes by object identity across frames to obtain, for each object o , a time-ordered track $\mathcal{T}_o = \{(b_i, t_i)\}_{i=1}^N$, where $b_i = [x_1^i, y_1^i, x_2^i, y_2^i]$ denotes the box at time t_i . From \mathcal{T}_o , we compute box centroids c_i and areas a_i , and use the induced displacement sequence $\Delta c_i = c_{i+1} - c_i$ to summarize motion.

We convert each track into a discrete motion descriptor consisting of direction, speed, and scale-change:

1. **Direction** is obtained by aggregating per-step displacement directions over the track (with weighting to reduce the influence of small localization jitter), and mapping the result to a finite set of compass bins plus a stationary state
2. **Speed** is computed from the track’s average displacement rate, normalized by an object-dependent scale factor (bounding box size) to be comparable across objects and videos, and discretized into ordinal bins
3. **Scale** is computed from the relative change in box area over time (a proxy for depth-like approach/recede behavior), and discretized into {approaching, stable, receding}

3.3 Training Pipeline

Our training follows the standard two-stage paradigm [5, 13] with minimal modifications, while introducing Motion-o as a format-level extension that explicitly supervises and rewards trajectory transition. We first teach the model to emit well-formed motion descriptors as part of the reasoning trace through supervised fine-tuning (SFT) and then directly optimize motion correctness and visual grounding through reinforcement learning (RL).

Stage 1: Supervised Fine-Tuning. We fine-tune Qwen2.5-VL-7B [1] on the motion-augmented STGR data described above. Using standard cross-entropy optimization, the model learns to produce `<motion/>` tags as a structured continuation of spatio-temporal evidence chains: after grounding multiple observations of an object with `<obj><box><t>`, it emits a self-closing `<motion obj="..." dir="..." speed="..." scale="..."/>` that summarizes the trajectory connecting those observations. Beyond offline data augmentation, the only additional requirement in this stage is a system prompt instruction that specifies the tag schema and allowed attribute values. This stage establishes (i) strict format validity (`<think>/<answer>` and tag well-formedness), (ii) spatio-temporal grounding syntax, and (iii) the motion descriptor schema, ensuring the policy enters RL with stable, parseable trajectory reasoning traces.

Stage 2: Reinforcement Learning. We build upon the training recipe in [13], adopting Group Sequence Policy Optimization (GSPO) [25] to stably optimize long-form evidence grounded video reasoning. Given a video-question prompt x , we sample a group of K candidate completions $\{y^{(k)}\}_{k=1}^K \sim \pi_\theta(\cdot | x)$, evaluate each completion with a scalar reward $r(x, y^{(k)})$ and compute a group-normalized advantage. GSPO then updates the policy using sequence-level importance ratios, which better aligns optimization with sequence-level rewards and improves stability for long-horizon reasoning.

Following [13], we decompose the scalar reward into three components:

$$r(x, y) = r_{\text{acc}}(x, y) + r_{\text{thk}}(x, y) + r_{\text{fmt}}(x, y). \quad (3)$$

where, r_{acc} encourages answer accuracy task-specific; e.g., exact match for MCQ, ROUGE for free-form QA), r_{fmt} enforces strict structured output formatting in the reasoning chain (including well-formed `<motion/>` tags), and r_{thk} incentivizes evidence-based reasoning. As in [13], we define the thinking reward as the sum of temporal and spatial grounding terms:

$$r_{\text{thk}}(x, y) = r_t(x, y) + r_s(x, y) + r_{\text{motion}}(x, y), \quad (4)$$

where r_t provides temporal supervision (with adaptive temporal proximity) and r_s provides spatial supervision with temporal gating to ensure spatial rewards are only computed when predicted timestamps are sufficiently close to ground-truth.

Motion-o extension: motion supervision inside r_{motion} . Our key extension is an explicit motion component

$$r_{\text{motion}}(x, y) = r_{\text{traj}}(x, y) + r_{\text{ground}}(x, y), \quad (5)$$

which teaches the model to (i) describe trajectory dynamics consistently with underlying tracks, and (ii) rely on true temporal evidence rather than textual priors.

Trajectory Reward. For each object tracked across at least two temporal observations, we compute ground-truth motion bins from the bounding box trajectory and score the model’s predicted `<motion/>` attributes via discrete bin matching with adjacency-aware partial credit:

$$r_{\text{traj}} = 0.4 \cdot r_{\text{dir}} + 0.3 \cdot r_{\text{speed}} + 0.3 \cdot r_{\text{scale}}. \quad (6)$$

Each attribute receives 1.0 for an exact match, 0.5 for an adjacent bin (direction: $\pm 45^\circ$; speed/scale: ± 1 ordinal rank), and 0.0 otherwise. Ground-truth bins are derived from centroid displacement and box area dynamics: direction from the dominant displacement vector quantized to eight compass points plus stationary, speed from displacement magnitude normalized by the object’s bounding box diagonal, and scale from the log-ratio of box areas between the first and last observation. Trajectory scores are computed per object identity to ensure consistency over a single track.

Visual Grounding Reward (Dual-Chain Verification). To encourage the model to derive motion descriptions from actual visual observation rather than textual interpolation, we introduce a visual grounding reward via dual-chain verification (see Stage 2 inputs in Figure 3). For each sample, we generate a second reasoning chain from a *motion-masked* version of the video (created by freezing frames to remove temporal motion cues). We then compare the `<motion/>` tags produced from the original video against those from the motion-masked input:

$$r_{\text{ground}} = 0.5 \mathbb{1}[d \neq d'] + 0.3 \mathbb{1}[s \neq s'] + 0.2 \mathbb{1}[c \neq c'], \quad (7)$$

where d, s, c and d', s', c' denote the direction, speed, and scale attributes from the original and masked outputs, respectively. If predicted motion changes when motion evidence is removed, the model exhibits dependence on temporal cues ($r_{\text{ground}} \rightarrow 1$); if predictions remain unchanged, it likely relies on non-visual shortcuts ($r_{\text{ground}} \rightarrow 0$). Objects absent from the motion-masked output are treated as fully grounded.

Synergy Between Trajectory and Visual Grounding Rewards. Both the trajectory and visual grounding reward enforce complementary requirements. The trajectory reward enforces *correctness* of motion descriptors with respect to ground-truth trajectories, while the visual grounding reward enforces *evidence dependence* on temporal visual information rather than textual anticipation. Correct motion reasoning (*e.g.*, predicting `dir="W"` when predicted boxes show leftward displacement) yields high r_{dir} ; accurate speed and scale descriptors align with bounding box predictions that match ground-truth velocity and area change, increasing r_{speed} and r_{scale} . Together they suppress two common failures: emitting `<motion/>` tags that are inconsistent with the underlying bounding box track, and emitting plausible `<motion/>` tags that could be produced without observing motion. This yields a self-reinforcing training signal: as the model learns to ground objects consistently across time, it is rewarded for emitting matching motion descriptors (higher r_{tra}); as it learns to rely on temporal evidence rather than priors, it is rewarded under motion masking (higher r_{ground}).

4 Experimental Results

4.1 Dataset

Dataset Augmentation: Trajectory Grounding with Dense Motion Annotations Existing spatio-temporal grounding datasets often provide bounding boxes at a small set of timestamps, yielding sparse trajectories that under-specify the motion connecting observations [13]. This sparsity is a bottleneck for motion reasoning: direction, speed, and scale are defined over continuous time, but supervision is provided only at isolated keyframes.

We densify sparse keyframe supervision on the Perception-LM (PLM) subset [3] by converting each sparse set of timestamped boxes into a temporally denser trajectory. For each tracked object, we preserve all original annotated keyframes

and insert intermediate supervision points at a fixed temporal stride between adjacent annotated timestamps. Intermediate bounding boxes are generated from interpolating the ground truth dense masks provided in the PLM dataset. This process converts originally sparse annotations into a dense per-object sequence of (t, b_t) pairs, substantially increasing temporal coverage for motion supervision. From the expanded trajectories, we compute object-level motion descriptors (see section 3.2 for details) and store them alongside the augmented tracks. Concretely, for each object we derive discrete attributes capturing (i) direction (quantized compass bins plus stationary), (ii) speed (binned using scale-normalized displacement), and (iii) scale change (binned from the area log-ratio trend), producing a compact summary of trajectory dynamics over the observed window. We then inject these descriptors directly into the model’s reasoning trace: after the final grounded mention of each object in the `<think>` chain (e.g., `<obj>... </obj><box>... </box> at <t>... </t>s`), we append a structured motion tag `<motion obj="..." dir="..." speed="..." scale="...">` that summarizes the object’s trajectory over the evidence window. This coupling ensures the model learns motion as *evidence-linked reasoning* rather than as an auxiliary label: the chain supervises not only *where* and *when* an object appears, but also *how* it evolves between observations. We release this augmentation as a standalone trajectory-grounding resource, including densely expanded trajectories, motion descriptors, and evaluation splits designed to isolate STT reasoning.

4.2 Setup

Base Models. We train Motion-o from Qwen2.5-VL-7B [1] following the two-stage pipeline in Sec. 3.3. To test whether MCoT provides additive gains on an already strong evidence-based model, we also add MCoT to the Open-o3 Video [13] checkpoint (denoted *Open-o3 + MCoT*). Both variants are evaluated with and without the visual grounding reward r_{ground} .

Benchmarks. Following Open-o3 Video [13], we report on the **V-STAR** benchmark [22] for spatio-temporal reasoning (What / When / Where, mAM, mLGM), and on **VideoMME** [6] and **WorldSense** [8] for general video understanding.

4.3 Main Results

Training Data.

V-STAR (Table 1). Open-o3 + MCoT achieves 36.6 mAM and 50.5 mLGM, improving over Open-o3 Video by +2.9 / +3.9 points. The gains are broad: What accuracy rises from 61.0 to 64.1, temporal grounding improves on both chains (Chain1: 24.5 \rightarrow 27.3, Chain2: 24.0 \rightarrow 26.8), and spatial grounding improves substantially (Chain1: 25.4 \rightarrow 33.6, Chain2: 6.0 \rightarrow 38.1), surpassing even the specialist Sa2VA-8B model on Where. Motion-o, trained from scratch on Qwen2.5-VL-7B, reaches 35.5 mAM, already surpassing Open-o3 Video and all open-source baselines. Removing r_{ground} reduces mAM by 0.5 for Motion-o and

Table 1: Performance on the **V-STAR** benchmark, which evaluates **spatio-temporal** reasoning across three dimensions. Chain1 denotes *what-when-where*; Chain2 corresponds to *what-where-when*. mAM is the average of arithmetic mean, and mLGM is the average of modified logarithmic geometric mean, combining temporal and spatial alignment. * indicates re-evaluation using the vLLM framework with 16 sampled frames. **Bold** numbers denote the best results, while underlined numbers indicate the second best.

Model	What	When (Temporal IoU)		Where (Visual IoU)		Overall	
	Acc	Chain1	Chain2	Chain1	Chain2	mAM	mLGM
GPT-4o	60.8	16.7	12.8	6.5	3.0	26.8	38.2
Gemini-2-Flash	53.0	24.5	23.8	4.6	2.2	26.9	35.6
Video-LLaMA3	41.9	23.0	23.1	0.9	0.2	21.7	27.0
LLaVA-Video	49.5	10.5	12.2	1.9	1.3	20.8	27.3
VideoChat2	36.2	13.7	12.5	2.5	1.0	17.0	20.3
Oryx-1.5-7B	20.5	13.5	14.8	10.1	3.5	15.1	13.8
InternVL-2.5-8B	44.2	8.7	7.8	0.7	0.1	17.6	24.9
Qwen2.5-VL-7B* (base)	33.5	15.4	13.8	17.0	2.5	19.3	22.4
TRACE	17.6	19.1	17.1	0.0	0.0	12.0	13.3
Sa2VA-8B	16.4	0.1	0.0	<u>32.3</u>	<u>37.5</u>	17.1	20.3
Open-o3 Video	61.0	24.5	24.0	25.4	6.0	33.7	46.6
Motion-o (w/o r_{ground})	62.2	26.2	25.8	26.6	12.3	35.0	48.8
Motion-o	62.7	<u>26.6</u>	<u>26.2</u>	28.2	15.1	<u>35.5</u>	<u>49.4</u>
Open-o3 + MCoT (w/o r_{ground})	<u>63.4</u>	26.3	25.6	30.5	31.4	35.2	49.1
Open-o3 + MCoT	64.1	27.3	26.8	33.6	38.1	36.6	50.5

1.4 for Open-o3 + MCoT, with the largest drops on spatial grounding, confirming that dual-chain verification is critical for visually grounded motion descriptions.

General Benchmarks (Table 2). Open-o3 + MCoT reaches 69.7 on VideoMME Overall and 41.5 on WorldSense, improving over Open-o3 Video by +6.1 and +4.0 points respectively while narrowing the gap with GPT-4o. Motion-o similarly improves over Qwen2.5-VL-7B across all metrics (+5.1 VideoMME, +3.1 WorldSense). These results confirm that explicit trajectory reasoning complements general video understanding rather than competing with it.

Qualitative Analysis. Figure 4 shows two representative outputs. In the first example, the model tracks Sheldon across three timestamps with varying camera angles and emits two <motion/> tags, both correctly identifying the subject as stationary despite significant viewpoint changes. The dense multi-point grounding enables the model to distinguish true stationarity from apparent visual displacement caused by camera cuts. In the second example, the model grounds a duck at four consecutive timestamps and summarizes its eastward trajectory with a single motion tag. Additional qualitative examples and analyses are provided in the supplementary material.

Table 2: Performance across video understanding and temporal grounding benchmarks. **Bold** numbers denote the best results, while underlined numbers indicate the second best.

Model	VideoMME		WorldSense	
	Overall	Long	Overall	Recognition
GPT-4o	71.9	-	42.6	-
Qwen2.5-VL-7B (base)	62.4	50.8	36.1	33.7
VideoRFT-7B	59.8	50.7	38.2	36.6
VideoR1-7B	61.4	50.6	35.5	32.8
Open-o3 Video	63.6	54.9	37.5	36.8
Motion-o (w/o r_{ground})	64.2	55.5	37.8	37.1
Motion-o	67.5	<u>58.6</u>	39.2	<u>38.5</u>
Open-o3 + MCoT (w/o r_{ground})	66.3	57.3	38.9	38.2
Open-o3 + MCoT	<u>69.7</u>	60.3	<u>41.5</u>	40.8

Table 3: Ablation on annotation density and tag representation (Motion-o, with r_{ground}). Dense/Discrete represents our default configuration.

Density	Tag Format	mAM	mLGM	VideoMME
<i>Annotation Density</i>				
Sparse	Discrete	31.2	44.5	68.1
Dense	Discrete	35.5	49.4	67.5
<i>Tag Representation (Dense)</i>				
Dense	Numerical	2.1	5.4	14.4
Dense	Discrete	35.5	49.4	67.5

4.4 Ablation Studies

Annotation Density (Table 3, top). Dense annotations improve mAM from 31.2 to 35.5 (+4.3) and mLGM from 44.5 to 49.4 (+4.9), confirming that denser bounding box tracks yield substantially stronger trajectory supervision. VideoMME remains comparable (68.1 vs. 67.5), indicating that density primarily benefits motion-specific reasoning without harming general understanding.

Tag Representation (Table 3, bottom). Replacing discrete bins with continuous numerical values (e.g., `speed="0.14 units/s"`, `accel="0.1"`) causes a near-complete collapse: mAM drops from 35.5 to 2.1 and VideoMME from 67.5 to 14.4. The model fails to learn meaningful structure from continuous motion values, confirming that discrete ordinal bins are essential; they provide a tractable vocabulary that the language model can reliably produce and that aligns naturally with the bin-matching reward.



Fig. 4: Qualitative examples of Motion-o reasoning. **Top:** The model tracks Sheldon across three timestamps with varying camera angles and emits two `<motion/>` tags, both correctly identifying the subject as stationary despite significant viewpoint changes. The dense multi-point grounding enables the model to distinguish true stationarity from apparent visual displacement caused by camera cuts. **Bottom:** The model grounds a duck at four consecutive timestamps as it swims through a group, summarizing the trajectory with a single motion tag capturing eastward direction at moderate speed.

5 Conclusion

We introduced Motion-o, a lightweight framework that makes motion dynamics explicit and verifiable in grounded video reasoning. Motion-o augments spatio-temporal evidence chains into spatial-temporal-trajectory evidence chains with MCoT: a structured `<motion/>` tag that bridges timestamped observations with object-conditioned motion attributes (direction, speed, scale). To provide supervision for these dynamics, we release a trajectory-grounding artifact that expands sparse keyframes into denser box tracks, and we train with complementary trajectory and visual grounding rewards that encourage motion tags to depend on temporal evidence. Across benchmarks, Motion-o improves trajectory-faithful reasoning without architectural changes, requiring only offline preprocessing and a small training-time overhead. More broadly, this work establishes a practical foundation for video understanding where reasoning is anchored in the explicit dynamics that make a video a video, enabling more reliable and interpretable motion-centric video models. Future work will explore extending MCoT to multi-object interactions, non-linear trajectories, and richer motion representations.

Supplementary Material

This supplementary document provides additional experimental details and extended results for **Motion-o**. We report (1) details on our training data for both supervised fine-tuning (SFT) and reinforcement learning (RL) stages (2) per-attribute accuracy of the `<motion/>` tag on our augmented trajectory-grounding dataset, (3) an ablation study on the trajectory reward weights, and (4) extended benchmark results on TVGBench [2], MVBench [10], and MotionBench [9].

6 Training Details

6.1 Training Data

Both Motion-o and Open-o3 + MCoT models reported in this paper are trained using data derived from the Spatio-Temporal Grounded Reasoning (STGR) dataset introduced in the Open-o3 paper [13]. Following that formulation, our training data is organized into SFT and RL stages, with each sample associated with a source dataset and a task type. The two models in this work, share the same RL data, but differ in their SFT mixtures to reflect different training priorities.

Shared RL data. For both Motion-o and Open-o3 + MCoT, the RL stage uses the same file, containing 34k training samples. This shared RL set includes five task categories: *temporal-spatial free-form QA* (12,047), *General video QA MCQ* (12,998), *visual QA* (5,000), *temporal QA* (2,279), and *general video QA free-form* (2,000). Using the same RL corpus for both models ensures that differences in final behavior are primarily attributable to the SFT data design rather than to different reinforcement learning supervision.

Motion-o SFT data. For Motion-o, the SFT stage uses a subset of the STGR dataset containing 22k samples. This mixture is broader and more balanced, combining motion-relevant grounded examples with a substantial amount of general video QA. Its task composition is: *general video QA free-form* (2,000), *General video QA MCQ* (13,000), *temporal QA* (491), and *temporal-spatial free-form QA* (7,047). This design preserves broad video reasoning coverage while still retaining a strong spatio-temporal grounding component, allowing Motion-o to couple explicit motion reasoning with more general video understanding capacity. Figure S5 summarizes the distribution of motion labels in our augmented dataset. Examples are not dominated by a single direction: eastward and westward motions are closely matched, and the remaining directional bins are also populated across the compass. This indicates that the learned `<motion/>` tags are trained on a reasonably balanced set of trajectory orientations, rather than reflecting a strong directional skew. The inner and outer rings further show that the data covers a range of speed and scale-change categories, providing supervision over multiple facets of motion behavior.

Open-o3 + MCoT SFT data. For Open-o3 + MCoT, we use the more motion-focused SFT mixture containing 7,838 samples. Its task composition is heavily concentrated in grounded motion-centric supervision: *temporal-spatial free-form QA* (6,849), *general video QA MCQ* (817), *general video QA free-form* (142), and *temporal QA* (30). We use this more concentrated SFT mixture for the Open-o3 + MCoT variant because the Open-o3 base model has already been exposed to the broader STGR-style training recipe, including SFT and RL on this same corpus family, in its original training pipeline [13]. Accordingly, for the MCoT variant we bias SFT more strongly toward motion-intensive grounded examples, with the goal of adapting the already grounded base model toward more explicit trajectory reasoning rather than repeating the full broad-coverage mixture used to establish its general grounded reasoning ability.

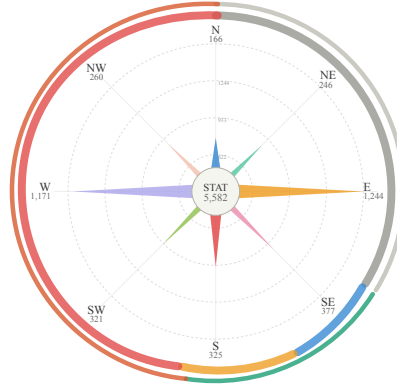


Fig. S5: Motion data compass showing the distribution of observations across direction, speed, and scale. Directional wedges radiate from the center using square-root scaling: **N** (166), **NE** (246), **E** (1,244), **SE** (377), **S** (325), **SW** (321), **W** (1,171), and **NW** (260); the central circle is stationary (5,582). The inner ring encodes speed: **stationary** (5,582), **slow** (1,396), **moderate** (1,266), **fast** (1,448). The outer ring encodes scale: **stable** (5,751), **approaching** (2,322), **receding** (1,619). Arc lengths are proportional to each category’s share.

Key difference in training emphasis. The main distinction between the two models lies in the SFT stage. Motion-o is trained with a larger and more mixed SFT corpus that retains substantial general video QA supervision alongside grounded spatio-temporal data, whereas Open-o3 + MCoT uses a smaller but much more concentrated motion-oriented SFT set. Motion-o prioritizes a balance between broad video reasoning competence and explicit motion-aware grounding, while Open-o3 + MCoT prioritizes targeted adaptation of an already grounded base model toward trajectory-explicit reasoning. This also explains why Open-o3 + MCoT achieves higher overall results: the Open-o3 base model has already been trained on the STGR corpus [13], giving it a strong prior over spatio-temporal grounding tasks. Our SFT stage therefore does not need to re-establish that general competence, and instead focuses narrowly on introducing `<motion/>` tag reasoning. The subsequent RL stage then builds directly on this foundation, using trajectory-consistency and visual grounding rewards to sharpen the model’s ability to produce track-consistent, explicitly grounded motion claims. The performance advantage of Open-o3 + MCoT thus reflects this compounding of a well-initialized base with targeted motion supervision, rather than any fundamental architectural difference.

Table S4: <motion/> tag accuracy on the augmented trajectory-grounding dataset. We report exact-match accuracy (%) for each motion attribute. “Avg” denotes the macro-average over three attributes.

Model	Direction	Speed	Scale	Avg
Motion-o (w/o r_{ground})	72.1	81.4	82.7	78.7
Motion-o (full)	78.9	88.3	88.4	85.2
Open-o3 + MCoT	74.8	84.2	85.6	81.5
Open-o3 + MCoT (w/ r_{ground})	80.4	90.7	90.1	87.1

6.2 Implementation Details

The SFT stage runs for 3 epochs on a single NVIDIA H200 GPU (140GB). The RL stage is conducted using 2 NVIDIA H200 GPUs (140GB).

7 Motion Tag Accuracy on the Augmented Dataset

Table S4 reports the per-attribute accuracy of predicted <motion/> tags against ground-truth motion descriptors computed from the dense bounding box tracks in our augmented dataset. We evaluate three attribute dimensions—direction (*dir*), speed, and scale, using both *exact match* (predicted bin equals the ground-truth bin) and *adjacent match* (predicted bin is within one ordinal step of ground truth, i.e. $\pm 45^\circ$ for direction and ± 1 rank for speed/scale). We report results for Motion-o (full model), the ablation without the visual grounding reward ($-r_{\text{ground}}$), and the Open-o3 + MCoT variant.

8 Extended Benchmark Results

Table S5 reports results on three additional benchmarks: **TVGBench** [2] for temporal video grounding, **MVBench** [10] for multi-modal video understanding, and **MotionBench** [9] (dev split) for motion-specific question answering. These complement the V-STAR, VideoMME, and WorldSense results in the main paper.

Quantitative Analysis The extended benchmark results in Table S5 show a clear and consistent pattern: making motion explicit improves performance not only on motion-focused benchmarks, but also on broader video reasoning tasks that implicitly depend on dynamic understanding. Starting from the Qwen2.5-VL-7B baseline, Motion-o improves TVGBench from 16.3 to 37.6 (+21.3) and MotionBench from 35.0 to 60.0 (+25.0). When added on top of the Open-o3 base model, the Open-o3 + MCoT (Motion Chain-of-Thought) variant further raises TVGBench from 20.8 to 39.6 (+18.8), MVBench from 64.4 to 69.2 (+4.8), and MotionBench from 45.0 to 63.0 (+18.0). Notably, the best variant also surpasses

the strongest open-source MVBench baseline in our table (69.2 vs. 67.9) and exceeds GPT-4o result on MotionBench by a wide margin (63.0 vs. 33.0). These gains suggest that explicit trajectory reasoning is improving a capability that many modern video benchmarks increasingly require. This pattern is important because the three benchmarks probe different surfaces of the same underlying problem. TVGBench emphasizes when evidence occurs and whether the model can temporally align its reasoning to the relevant segment. MotionBench is more directly motion-centric, explicitly testing categories such as action order, camera motion, location-related motion, and motion recognition. MVBench is broader and more heterogeneous, but many of its subsets also depend strongly on dynamics rather than static appearance alone, including action sequence, action prediction, and object interaction. Benchmarks are increasingly converging toward testing a model’s ability to reason about temporal change, transitions, and object evolution, rather than merely recognizing static content.

The key point we want to emphasize here is that benchmark construction has already started moving in a motion-centric direction, but most models have not. Many recent methods are designed as generic video reasoners: they may improve temporal grounding, spatial localization, or chain-of-thought style inference, but they still do not explicitly model the trajectory that connects observations. Existing evidence-based video reasoning frameworks have become increasingly strong at grounding where an object is and when it appears, yet they typically leave how it moved between those observations implicit. This forces the model to interpolate dynamics internally, often relying on priors, textual smoothness, or weakly grounded heuristics rather than an explicit motion representation. Motion-o directly targets this gap by introducing with the structured `<motion/>` tag that summarizes direction, speed, and scale change between grounded observations, turning trajectory reasoning into an explicit and rewardable intermediate step. The gains do not come from architectural novelty, but from changing what the model is required to represent. Motion-o changes the supervision target and the reward structure so that motion is no longer an implicit byproduct of spatio-temporal grounding, but an explicit reasoning primitive. Prior models may include motion-sensitive metrics or temporal supervision, but the models themselves do not articulate motion patterns in their reasoning traces. In Motion-o, the trajectory is part of the reasoning trace itself, and the RL stage further encourages those motion claims to be both track-consistent and visually grounded under motion masking.

Qualitative Analysis Figure S6 highlights a successful case where Motion-o captures a subtle but important temporal pattern: the baby moves in one circular direction and later reverses direction. In the generated reasoning trace, the motion grounding reflects this change explicitly, first marking the baby with westward motion and later with eastward motion. This example is qualitatively important because the key evidence is not merely the baby’s presence or spatial location, but the change in trajectory over time. The model does not rely only on static snapshots; instead, it uses motion-grounded evidence across timestamps to support the answer. This illustrates the central motivation of Motion-o: making

Table S5: Extended benchmark results. We report accuracy on TVGBench (mIoU), MVBench, and MotionBench (Overall accuracy, dev split). Best open-source results in **bold**.

Model	TVGBench [2]	MVBench [10]	MotionBench [9]
<i>Proprietary models</i>			
GPT-4o	-	-	33.0
<i>Open-source models</i>			
Qwen2.5-VL-7B	16.3	66.9	35.0
Video-R1-7B	9.6	62.7	-
VideoChat-R1-7B	-	67.9	-
Open-o3 Video-7B	20.8	64.4	45.0
<i>Ours</i>			
Motion-o (w/o r_{ground})	35.6	65.2	55.0
Motion-o (full)	37.6	65.8	60.0
Open-o3 + MCoT	38.2	67.2	60.0
Open-o3 + MCoT (w/ r_{ground})	39.6	69.2	63.0

trajectory evolution explicit allows the model to reason about dynamic events that would otherwise remain implicit in standard spatio-temporal grounding pipelines. In this case, the model correctly tracks the temporal progression of the action and exposes the reversal through the structured motion tag, showing that the proposed motion-centric reasoning pathway can capture directional transitions that are essential for true video understanding.

Figure S7 illustrates an important limitation of the current approach. Although the model arrives at the correct motion understanding the spatial localization is weak, as the predicted boxes do not tightly align with the referenced objects. This behavior is consistent with the design of the system. In the current pipeline, bounding boxes are produced by the underlying VLM backbone (here, Qwen), which is not a native object detector and is therefore not optimized for precise localization. As a result, Motion-o can still leverage coarse grounding and motion-aware reasoning to reach the correct answer, but the visual grounding itself may be spatially noisy. This suggests a natural direction for future improvement. One promising extension would be to integrate a stronger spatial localization component, such as a dedicated detector or grounding module, so that trajectory reasoning can operate on more accurate object tracks.

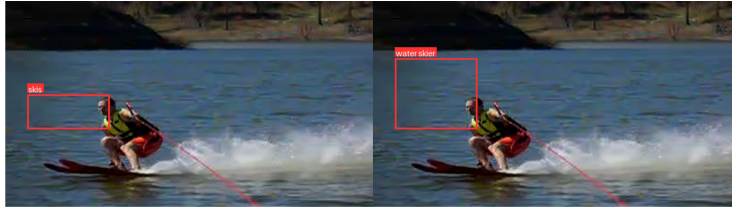


Question: Who does the adult hold the hand of?

Reasoning: The video shows an adult helping a baby learn to walk. At the beginning of the clip, the `<obj>baby</obj><box>[223,130,370,340]</box>at<t>1.5</t>s` is holding onto the adult's hands for support as they take their first steps. As the baby continues to practice walking, the adult holds the baby's hands to help them maintain balance. For instance, the `<obj>baby</obj><box>[223,130,370,340]</box>at<t>3.0</t>s<motion obj="baby" dir="W" speed="slow" scale="stable"/>` is still holding the adult's hands while learning to walk. This interaction continues throughout the segment, as seen again when the `<obj>baby</obj><box>[223,130,370,340]</box>at<t>12.0</t>s<motion obj="baby" dir="E" speed="slow" scale="stable"/>` is holding the adult's hands. Therefore, the adult is holding the hand of the baby.

Answer: The adult holds the hand of a baby.

Fig. S6: Qualitative example showing successful motion-centric reasoning: the model captures the baby's change in movement direction over time through explicit motion grounding.



Question: What is beneath the adult wearing red pants?

Reasoning: The video shows an adult water skiing on a body of water. The adult is wearing red pants and a life vest while being pulled by a rope attached to a boat. Throughout the segment, the `<obj>water skier</obj><box>[38,101,181,224]</box>at<t>1.7</t>s` is seen gliding over the surface of the water. The water skier's feet are firmly planted on the `<obj>skis</obj><box>[38,164,181,224]</box>at<t>1.7</t>s<motion obj="skis" dir="W" speed="slow" scale="stable"/>`, which are positioned directly above the water. This visual evidence confirms that the water skier is standing on the skis, which are on the water.

Answer: The adult is standing on a pair of skis, which are on the water.

Fig. S7: Qualitative limitation example: the model reaches the correct answer, but the spatial grounding is imprecise, highlighting the need for stronger localization modules.

References

1. Bai, S., Chen, K., Liu, X., Wang, J., Ge, W., Song, S., Dang, K., Wang, P., Wang, S., Tang, J., et al.: Qwen2.5-vl technical report. arXiv preprint arXiv:2502.13923 (2025)
2. Chen, R., Luo, T., Fan, Z., Zou, H., Feng, Z., Xie, G., Zhang, H., Wang, Z., Liu, Z., Huaijian, Z.: Datasets and recipes for video temporal grounding via reinforcement learning. In: Proceedings of the 2025 Conference on Empirical Methods in Natural Language Processing: Industry Track. pp. 983–992 (2025)
3. Cho, J.H., Madotto, A., Mavroudi, E., Afouras, T., Nagarajan, T., Maaz, M., Song, Y., Ma, T., Hu, S., Jain, S., et al.: Perceptionlm: Open-access data and models for detailed visual understanding. In: The Thirty-ninth Annual Conference on Neural Information Processing Systems (2025)
4. Fan, Y., He, X., Yang, D., Zheng, K., Kuo, C.C., Zheng, Y., Guan, X., Wang, X.E.: Grit: Teaching mllms to think with images. In: The Thirty-ninth Annual Conference on Neural Information Processing Systems (2025)
5. Feng, K., Gong, K., Li, B., Guo, Z., Wang, Y., Peng, T., Wu, J., Zhang, X., Wang, B., Yue, X.: Video-r1: Reinforcing video reasoning in mllms. arXiv preprint arXiv:2503.21776 (2025)
6. Fu, C., Dai, Y., Luo, Y., Li, L., Ren, S., Zhang, R., Wang, Z., Zhou, C., Shen, Y., Zhang, M., et al.: Video-mme: The first-ever comprehensive evaluation benchmark of multi-modal llms in video analysis. In: Proceedings of the IEEE/CVF conference on computer vision and pattern recognition. pp. 24108–24118 (2025)
7. Gu, X., Zhang, H., Fan, Q., Niu, J., Zhang, Z., Zhang, L., Chen, G., Chen, F., Wen, L., Zhu, S.: Thinking with bounding boxes: Enhancing spatio-temporal video grounding via reinforcement fine-tuning. arXiv preprint arXiv:2511.21375 (2025)
8. Hong, J., Yan, S., Cai, J., Jiang, X., Hu, Y., Xie, W.: Worldsense: Evaluating real-world omnimodal understanding for multimodal llms. arXiv preprint arXiv:2502.04326 (2025)
9. Hong, W., Cheng, Y., Yang, Z., Wang, W., Wang, L., Gu, X., Huang, S., Dong, Y., Tang, J.: Motionbench: Benchmarking and improving fine-grained video motion understanding for vision language models. In: Proceedings of the Computer Vision and Pattern Recognition Conference. pp. 8450–8460 (2025)
10. Li, K., Wang, Y., He, Y., Li, Y., Wang, Y., Liu, Y., Wang, Z., Xu, J., Chen, G., Luo, P., et al.: Mvbench: A comprehensive multi-modal video understanding benchmark. In: Proceedings of the IEEE/CVF Conference on Computer Vision and Pattern Recognition. pp. 22195–22206 (2024)
11. Li, X., Yan, Z., Meng, D., Dong, L., Zeng, X., He, Y., Wang, Y., Qiao, Y., Wang, Y., Wang, L.: Videochat-r1: Enhancing spatio-temporal perception via reinforcement fine-tuning. arXiv preprint arXiv:2504.06958 (2025)
12. Liu, Y., Li, S., Liu, Y., Wang, Y., Ren, S., Li, L., Chen, S., Sun, X., Hou, L.: Tempcompass: Do video llms really understand videos? arXiv preprint arXiv:2403.00476 (2024)
13. Meng, J., Li, X., Wang, H., Tan, Y., Zhang, T., Kong, L., Tong, Y., Wang, A., Teng, Z., Wang, Y., et al.: Open-o3 video: Grounded video reasoning with explicit spatio-temporal evidence. arXiv preprint arXiv:2510.20579 (2025)
14. OpenAI: Introducing o3 and o4-mini. <https://openai.com/index/introducing-o3-and-o4-mini/> (2025)
15. Ouyang, K., Liu, Y., Wu, H., Liu, Y., Zhou, H., Zhou, J., Meng, F., Sun, X.: Spacer: Reinforcing mllms in video spatial reasoning. arXiv preprint arXiv:2504.01805 (2025)

16. Park, J., Na, J., Kim, J., Kim, H.J.: Deepvideo-r1: Video reinforcement fine-tuning via difficulty-aware regressive grpo. In: NeurIPS (2025)
17. Varma, M., Delbrouck, J.B., Ostmeier, S., Chaudhari, A.S., Langlotz, C.: TRove: Discovering error-inducing static feature biases in temporal vision-language models. In: The Thirty-ninth Annual Conference on Neural Information Processing Systems (2025)
18. Wang, H., Li, X., Huang, Z., Wang, A., Wang, J., Zhang, T., Bai, S., Kang, Z., Feng, J., Zhuochen, W., et al.: Traceable evidence enhanced visual grounded reasoning: Evaluation and method. In: The Fourteenth International Conference on Learning Representations (2026)
19. Wang, J., Kang, Z., Wang, H., Jiang, H., Li, J., Wu, B., Wang, Y., Ran, J., Liang, X., Feng, C., et al.: Vgr: Visual grounded reasoning. arXiv preprint arXiv:2506.11991 (2025)
20. Wang, Q., Yu, Y., Yuan, Y., Mao, R., Zhou, T.: Videorft: Incentivizing video reasoning capability in mllms via reinforced fine-tuning. In: The Thirty-ninth Annual Conference on Neural Information Processing Systems (2025)
21. Wang, Y., Wang, Z., Xu, B., Du, Y., Lin, K., Xiao, Z., Yue, Z., Ju, J., Zhang, L., Yang, D., et al.: Time-r1: Post-training large vision language model for temporal video grounding. In: The Thirty-ninth Annual Conference on Neural Information Processing Systems (2026)
22. Wang, Y., Zheng, Z., Zhao, X., Li, J., Wang, Y., Zhao, D.: Vstar: A video-grounded dialogue dataset for situated semantic understanding with scene and topic transitions. In: Proceedings of the 61st Annual Meeting of the Association for Computational Linguistics (Volume 1: Long Papers). pp. 5036–5048 (2023)
23. Wang, Z., Yoon, J., Yu, S., Islam, M.M., Bertasius, G., Bansal, M.: Video-rts: Rethinking reinforcement learning and test-time scaling for efficient and enhanced video reasoning. In: Proceedings of the 2025 Conference on Empirical Methods in Natural Language Processing. pp. 28114–28128 (2025)
24. Zhang, X.: The escalator problem: Identifying implicit motion blindness in ai for accessibility. In: Proceedings of the IEEE/CVF International Conference on Computer Vision (ICCV) Workshops. pp. 6635–6643 (October 2025)
25. Zheng, C., Liu, S., Li, M., Chen, X.H., Yu, B., Gao, C., Dang, K., Liu, Y., Men, R., Yang, A., et al.: Group sequence policy optimization. arXiv preprint arXiv:2507.18071 (2025)
26. Zheng, Z., Yang, M., Hong, J., Zhao, C., Xu, G., Yang, L., Shen, C., Yu, X.: Deepeyes: Incentivizing thinking with images via reinforcement learning. arXiv preprint arXiv:2505.14362 (2025)